ISSN 1068-1620, Russian Journal of Bioorganic Chemistry, 2017, Vol. 43, No. 3, pp. 235–247. © Pleiades Publishing, Ltd., 2017.
Original Russian Text © T.A. Gudasheva, A.V. Tarasiuk, N.M. Sazonova, S.V. Pomogaibo, A.N. Shumskiy, I.O. Logvinov, S.V. Nikolaev, P.Yu. Povarnina, M.A. Konstantinopolsky, T.A. Antipova, S.B. Seredenin, 2017, published in Bioorganicheskaya Khimiya, 2017, Vol. 43, No. 3, pp. 236–249.

Design, Synthesis, and Neuroprotective Effects of a Dimeric Dipeptide Mimetic of the Third Loop of the Nerve Growth Factor

T. A. Gudasheva[1], A. V. Tarasiuk, N. M. Sazonova, S. V. Pomogaibo, A. N. Shumskiy, I. O. Logvinov, S. V. Nikolaev, P. Yu. Povarnina, M. A. Konstantinopolsky, T. A. Antipova, and S. B. Seredenin

Zakusov Research Institute of Pharmacology, Moscow, 125315 Russia

Received May 11, 2016; in final form, June 6, 2016

Abstract—Previously, we prepared dimeric dipeptide mimetics of the first and the fourth loops of the nerve growth factor (NGF): hexamethylenediamides of bis(*N*-aminocaproyl-glycyl-L-lysine) (GK-6) and bis(*N*-monosuccinyl-L-glutamyl-L-lysine) (GK-2). Both mimetics activated TrkA-receptors, but induced different postreceptor signal pathways. GK-2 selectively activated PI3K/AKT, whereas GK-6 activated both PI3K/AKT and MAPK/ERK. Both mimetics exhibited a neuroprotective activity. In this study, we continued the investigation of a contribution of separate loop-like structures in the NGF functions and created and studied dimeric dipeptide mimetics based on a beta-turn of the NGF third loop: hexamethylenediamides of bis(*N*-gamma-hydroxybutyryl-L-lysyl-L-histidine) (GTS-115) and bis(*N*-acetyl-L-lysyl-L-histidine) (GTS-113). GTS-115 was shown to exhibit the neuroprotective activity in the concentration range from 10^{-5} to 10^{-7} M towards the HT-22 cell culture under the conditions of oxidative stress. The acetyl-containing GTS-113 mimetic proved to be inactive. GTS-115 (1 mg/kg/day intraperitoneally, for 7 days, the administration was started 4 h after the operation) exhibited the neuroprotective properties and decreased the infarction volume by 25% on the model of a stroke that was induced by a transient occlusion of the medial cerebral artery of rats. The action mechanism of GTS-115 was studied by Western-blot analysis and this mimetic in a concentration of 10^{-6} M was shown to activate the TrkA-receptor and both MAPK/ERK and PI3K/AKT basic postreceptor signal pathways. The inhibitory analysis revealed different contributions of these pathways into the GTS-115 neuroprotective effect. The LY294002 selective inhibitor of PI3K completely blocked the neuroprotective effect of GTS-115 in vitro, whereas the PD98059 specific inhibitor of MEK1 and MEK2 decreased this effect only by 10–15%. GTS-115 peptide stimulated a differentiation of the PC12 cells and caused a hyperalgesia in rats. These facts were in a good agreement with the literature data on the participation of the MAP-kinase pathway in these effects. Thus, the third NGF loop and the neighboring first NGF loop activated the postreceptor pathways in a similar way and exhibited the similar activities.

Keywords: NGF, mimetic, the GTS-115 dipeptide, neuroprotective activity, MAPK/ERK, PI3K/AKT

DOI: 10.1134/S1068162017030050

INTRODUCTION

The nerve growth factor (NGF) is the first from the neurotrophine family. It was discovered in the 50s of the 20th century and, since that time, has attracted attention as a possible drug for a treatment of neurodegenerative diseases [1]. However, it has found only a limited application in clinical practice due to its poor stability in biological liquids, poor ability to penetrate through the blood-brain barrier (BBB), and serious side effects, especially hyperalgesia [2]. Thus, the search for low-molecular weight compounds which will exhibit the therapeutically promising effects of NGF but will be free from the disadvantages of the full-size protein is a topical problem.

[1] Corresponding author: phone: +7 (495) 601-2246; +7 (916) 803-33-35, e-mail: tata-sosnovka@mail.ru.

Abbreviations: BuONO, *n*-butyl nitrite; DCC, 1,3-dicyclohexylcarbodiimide; DCU, 1,3-dicyclohexylurea; DIEA, *N*,*N*-diisopropylethylamine; DMAPA, 3-(dimethylamino)propylamine; GHB, gamma–hydroxybutyric acid; MAPK/ERK, the mitogen-activated proteinkinase pathway; NGF, the nerve growth factor; PI3K/AKT, phosphatidyl inositol-3-kinase pathway; TEA, triethylamine; TFA, trifluoroacetic acid.

NGF is a homodimer with each protomer that consists of 118 aa. These 118-member protomers are arranged in 7 beta-strands which are interconnected with four disordered regions called loops. Since they are most exposed to a solvent, many researchers believe that precisely these loops participate in the NGF interaction with the specific TrkA-receptor, subsequently induce the receptor dimerization, autophosphorylation, and activation of several signal pathways, including the phosphatidylinositol-3-kinase (PI3K/AKT) and the mitogen-activated proteinkinase (MAPK/ERK) pathways. The MAPK pathway is known to be generally responsible for the cell differentiation and to be involved in the hyperalgesia, whereas the AKT pathway is mainly responsible for the neuroprotection [3, 4].

The hypothesis that the different neurotrophine functions were controlled by the interaction of the different loops with the same Trk receptor was proposed in the Zakusov Research Institute of Pharmacology [5]. The hexamethylenediamide of bis(*N*-monosuccinyl-L-glutamyl-L-lysine) and hexamethylenediamide of bis(*N*-aminocaproylglycyl-L-lysine) dipeptide dimeric mimetics of the fourth and the first loops of NGF (GK-2 and GK-6, respectively) were created to confirm this hypothesis [6]. The main idea of these constructs was the preservation of the central fragment of the beta-turn and substitution of bioisosteric residue for the preceding residue. The NGF-like dimer was prepared with the use of a symmetric spacer [5]. Both mimetics activated the TrkA receptors and exhibited the neuroprotective activity in vitro in micromolar or nanomolar concentrations. The neuroprotective effects of GK-2 were confirmed in the in vivo experiments [7, 8]. The detailed investigation of the mechanism of action demonstrated that both mimetics interacted with TrkA, but induced different postreceptor signal pathways. GK-6 activated the ERK and AKT signal pathways, whereas GK-2 initiated only the AKT pathway. GK-6, distinct from GK-2, also exhibited the differentiating activity and caused hyperalgesia in rats [9].

In this study, we synthesized and studied mimetics of the third loop of NGF.

RESULTS AND DISCUSSION

Design and Synthesis of the NGF Mimetics

The spatial structure of the nerve growth factor (PDB ID: 1BET) was used for the design of the NGF mimetics. According to the previously proposed hypothesis about a key role of central fragments of beta-turns of the loops in the neurotrophin activity [5], the beta-turn of the third loop that contained the -Ser^{73}-Lys^{74}-His^{75}-Trp^{76}- fragment was chosen for the mimetic design. We preserved the amino acid residues of the central fragment (-Lys^{74}-His^{75}-) in the mimetic structure. From geometrical considerations, side chains of these residues could most deeply penetrate the receptor binding site and be best recognized by the receptor. The peripheral Ser^{73} residue was replaced by the bioisosteric residue of gamma-hydroxybutyric acid (GHB), and the amide group was introduced instead of the Trp^{76} residue. These two substitutions were made with the aim of stabilization of the beta-turn conformation, increase in the resistance of the compound to the peptidase attacks, and a reduction in the synthesis price.

Since NGF interacted with the receptor as the homodimer [3], we synthesized a homodimeric form from two mimetics of the beta-turn which were connected with each other "head-to-head" through the hexamethylene spacer in order to prepare a compound with the agonistic activity. Thus, the dimeric dipeptide mimetic (GTS-115) of the third neurotrophin loop, hexamethylenediamide of bis(*N*-gamma-hydroxybutyryl-L-lysyl-L-histidine) was created. The GTS-113 mimetic, hexamethylenediamide of bis(N-acetyl-L-lysyl-L-histidine), without the serine side chain in the *N*-acyl radical was prepared to elucidate the role of the Ser^{73} residue of the third loop of the beta-turn (gamma-hydroxybutyryl residue of GTS-115) in the neuroprotective effect of the neurotrophin.

The GTS-113 and GTS-115 peptides were prepared by the conventional peptide synthesis in solution using the Z/Boc-protection strategy. The amino acid residues were attached by the method of active *N*-hydroxysuccinimide esters. The *N*-protected dipeptide was condensed with hexamethylenediamine by the azide method. The target compounds were obtained as their hydrochlorides (see the scheme).

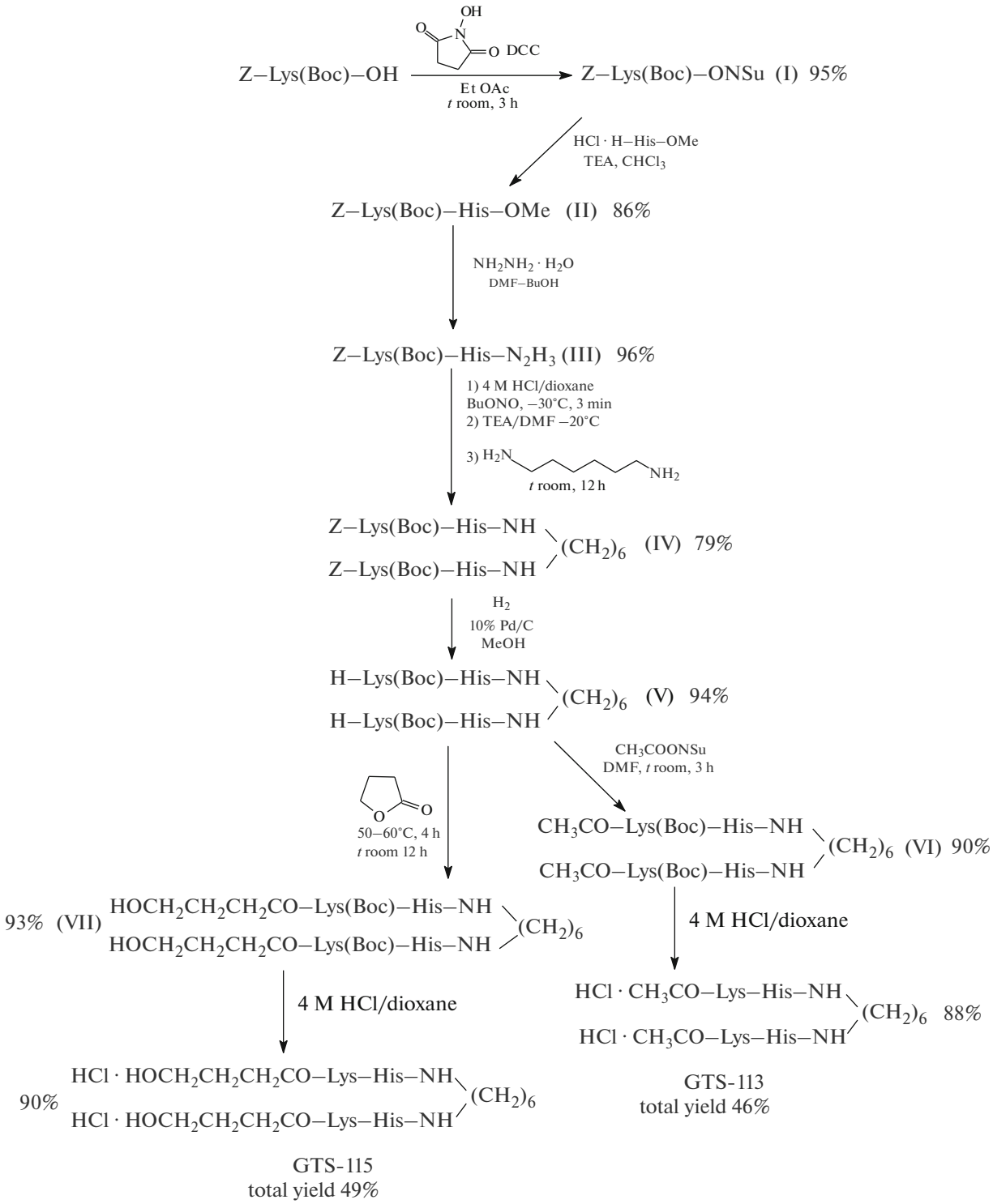

Scheme. Synthesis of the GTS-113 and GTS-115 mimetics of the third loop of NGF.

First, the active *N*-hydroxysuccinimide ester of the protected lysine, Z-Lys(Boc)-ONSu (**I**), was synthesized with a yield of 95%. A condensation of this active ester with the histidine methyl ester resulted in the methyl ester of dipeptide (**II**) with a yield of 96%. The dipeptide was further converted into the corresponding hydrazide (**III**) by the treatment with hydrazine hydrate in methanol. Hydrazide (**III**) was treated with *n*-butyl nitrite in an acidic medium and the resulting azide was immediately condensed with hexamethylenediamine to give hexamethylenediamide of the bis-dipeptide (Z-Lys(Boc)-His-NH-)$_2$(CH$_2$)$_6$ (**IV**) with a

yield of 79%. The Z-protecting group was removed by the catalytic hydrogenolysis in the presence of palladium on the active coal, and the obtained product (**V**) was treated with butyrolactone at 50–60°C. The acylated product (**VI**) was subjected to acydolysis in 4 M HCl in dioxane. GTS-115 was obtained as its hydrochloride with the total yield of 46%. GTS-113 was prepared by the addition of *N*-hydroxysuccinimide ester of acetic acid to the early obtained bisdipeptide (**V**) in DMF. Product (**VII**) was subjected to acydolysis in 4 M HCl in dioxane, and GTS-113 was obtained as its hydrochloride with the total yield 43%.

The structure and the diasteriomeric homogeneity of GTS-113, GTS-115, and all the intermediate products were confirmed by ^{1}H NMR spectroscopy. The substances were characterized by the values of their chromatographic mobility in a thin layer of the silica gel in various solvent systems and their physicochemical constants (mp and $[\alpha]_D$).

Studies of the Neuroprotective Activity in vitro

The neuroprotective activity of the synthesized GTS-113 and GTS-115 dipeptides was examined on the model of the hydrogen-peroxide-induced oxidative stress on the culture of the mouse immortalized hippocampal cells of the HT-22 line [10] in the concentration interval from 10^{-5} to 10^{-8} M (see Fig. 1).

GTS-115 exhibited the neuroprotective activity in the concentration range from 10^{-5} to 10^{-7} M. The GTS-113 acetyl-containing mimetic which was distinguished from GTS-115 only by the absence of hydroxyethyl radical was inactive. Based on this data, we could conclude that the residue of gamma-hydroxybutyric acid was necessary for the GTS-115 neuroprotective activity, and, thus, the Ser73 residue played an important role in NGF.

Studies of the Mechanism of Action of the GTS-115 Mimetic

NGF is well known to exhibit its basic biological functions, in particular neuroprotection and differentiating activity, through its interaction with the TrkA receptors with the subsequent induction of the main PI3K/AKT and MAPK/ERK postreceptor signal cascades. We investigated a possible influence of the GTS-115 mimetic of the third NGF loop in its most active concentration (10^{-6} M) on a phosphorylation of the TrkA, AKT, and ERK kinases in hippocampal neurons of the HT-22 line by Western-blot analysis using monoclonal antibodies to the phosphorylated and nonphosphorylated forms of these kinases.

GTS-115 in a concentration of 10^{-6} M activated the TrkA receptor and both signal pathways of the AKT and ERK kinases (see Fig. 2). The significant increase in the phosphorylation of the TrkA receptor and the AKT kinases was observed 30, 60, and 180 min after incubation with mimetic. The phosphorylation of the ERK kinases increased after 30 and 60 min incubation.

The kinase activation pathways which were involved into the neuroprotective activity of the GTS-115 mimetic were revealed with the application of the LY294002 inhibitor of the phosphatidylinositol-3-kinase in a concentration of 10^{-4} M and the PD98059 specific inhibitor of the MEK1 and MEK2 mitogen-activated proteinkinases in a concentration of 0.5×10^{-4} M (see Fig. 3).

The addition of LY294002 completely prevented a development of the neuroprotective effect of GTS-115 in both experimental schemes (the peptide administration 24 h before the damage of just after the damage). At the same time, the inhibition of the activity of the ERK-specific mitogen-activated MEK proteinkinase by the PD98059 specific inhibitor resulted in only a 10–15% decrease in the neuroprotective effect of GTS-115 (Fig. 4). Our results confirmed the literature data [11] on the most important role of the PI3K/AKT kinase pathway in the development of the neuroprotective effect.

The differentiating activity of NGF is known to be associated with the MAP-kinase pathway [3]. The differentiating activity of GTS-115 was examined on the culture of pheochromocytoma cells of the PC12 line which contained the TrkA receptors and was differentiated according to the neuronal type [12] after the NGF addition (Fig. 5).

GTS-115 was found to stimulate the axon growth in the PC12 cells similarly to NGF. GTS-115 was active in all the range of the studied concentrations (from 10^{-5} to 10^{-8} M).

Investigation of the Neuroprotective Activity of GTS-115 In Vivo

The neuroprotective properties of GTS-115 were studied on a model of the ischemic stroke which was caused by a transient occlusion of the rat medial cerebral artery [13]. The substance was intraperitoneally administered at a dose of 1 mg/kg for 7 days.

The GTS-115 treatment resulted in an improved neurologic status of the animals even on the third day after the operation. The therapeutic effect of GTS-115 proved to be approximately 40% according to the limb-placing test [14, 15].

The morphometric analysis of the brain sections demonstrated that the volume of the infarction zone of the animals in the "stroke" group was about 300 mm^3. The GTS-115 treatment resulted in a decrease in the volume of this zone by 25% (Fig. 6).

Thus, GTS-115 exhibits the neuroprotective properties both in vitro and in vivo on the model of the stroke which is caused by the transient occlusion of the medial cerebral artery.

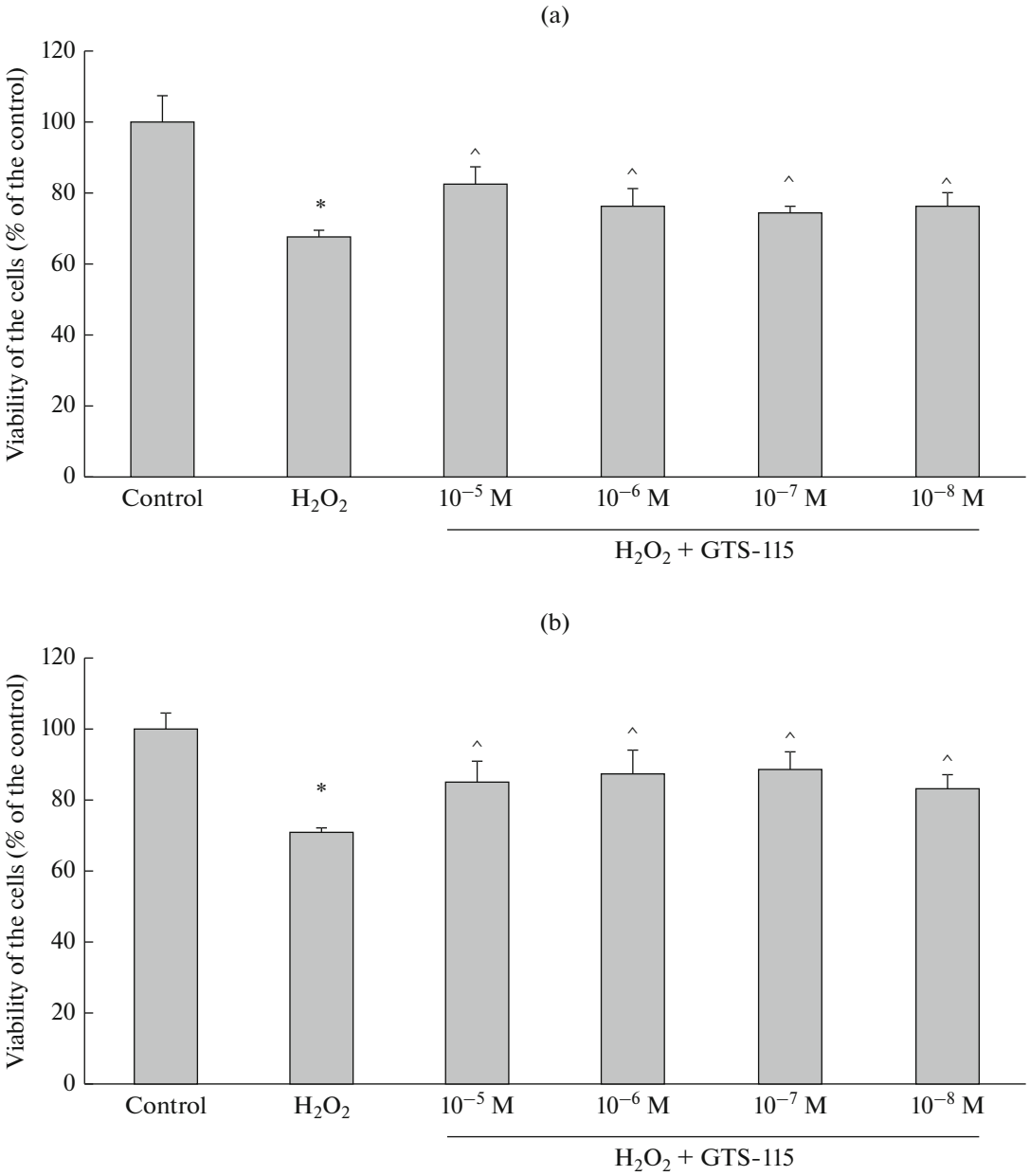

Fig. 1. The neuroprotective activity of the GTS-115 mimetic of the third loop of NGF on the model of the oxidative stress in the culture of the hippocampal neurons of the HT-22 line at (a) the GTS-115 administration 24 h before the damage and (b) just after the damage. The data are given as mean deviation and roof-mean-square deviation. *$p < 0.01$ in comparison with the control, ^$p < 0.05$ in comparison with the injury (the Mann-Whitney U-test).

Side effects of GTS-115

The main side effects of NGF are known to be a hyperalgesia [16] and a body weight loss [17]. In this connection, the influence of the GTS-115 active mimetic of the third NGF loop on the pain threshold and the rat body weight has been studied.

The *GTS-115 influence on the pain threshold* of rats was examined in the "hot plate" test [18]. The GTS-115 effect was evaluated 24 h after its administration similarly to NGF. No statistically significant differences in the time of the rat reaction to the thermic stimulus were revealed at the point of measurement (0 and 24 h). The average time of the reaction to the thermic stimulus was 5.83 ± 0.21 s before the GTS-115 administration (0.1 mg/kg, intraperitoneally) and 4.35 ± 0.27 s after the peptide administration. Thus, GTS-115 significantly decreased ($p < 0.05$) the rat pain threshold (by 25%) in comparison with the initial

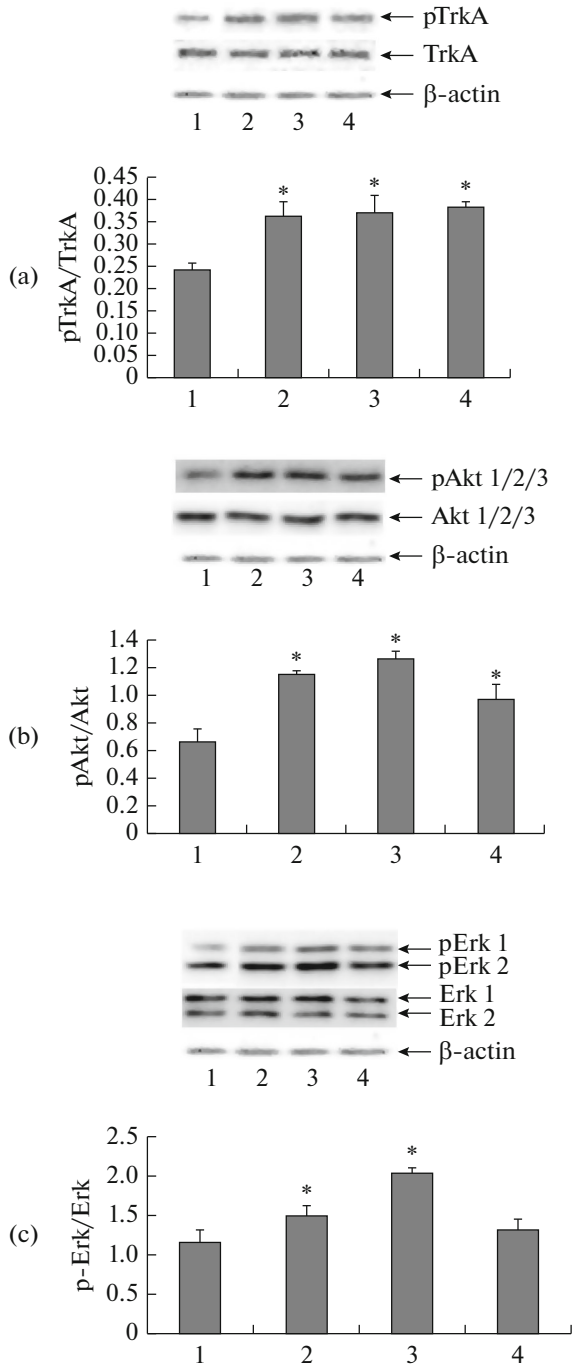

Fig. 2. GTS-115 stimulates phosphorylation of (a) TrkA receptor, (b) Akt kinase, and (c) Erk kinase. The kinase phosphorylation was studied on the hippocampal neurons of the HT-22 line by the Western-blot analysis using the specific antibodies to phosphorylated and nonphosphorylated forms of the corresponding kinases. The content of the phosphorylated kinases was determined (2) 30, (3) 60, and (4) 180 min after the addition of GTS-115 in the final concentration of 10^{-6} M in the culture medium. The original Western-blots and the results of densitometry were given. The data were presented as mean deviations and root-mean-square deviations of the ratios of the optic density of the Western-blots of the phosphorylated forms to those of the nonphosphorylated forms. Line 1 corresponded to the control. *$p < 0.95$ relatively to the control (the Mann-Whitney U-test). Beta-actin was used as a loading control protein.

level, suggesting the NGF-like hyperalgesic activity of GTS-115 [2].

The possible *influence of GTS-115 on the body weight* was studied at its daily intraperitoneal administration to outbred male rats for 14 days at a dose of 1 mg/kg. No differences in the body weight were found between the animals with were treated with the NGF mimetic and distilled water during this experiment, i.e., GTS-115 did not affect the rat body weight.

Thus, the studies of biochemical and pharmacological properties of the mimetic of the third NGF loop and the comparison of the data with those for the previously investigated mimetics of the first and the fourth loops of NGF [9] demonstrate the similar picture of the activation of the postreceptor pathways. Moreover, the activity spectra of the neighboring third and first loops of NGF prove to be analogous (the table).

EXPERIMENTAL

The commercially available amino acids and their derivatives (Reanal, Flucka, and Merck) were used in this study. The solvents were purified and dried according to the standard methods. ^{1}H and ^{13}C NMR spectra (δ, ppm; *J*, Hz) were recorded on a Fourier-300 spectrometer (Bruker, Germany) in the solutions in DMSO-d_6 and D_2O. Tetramethylsilane was used as an internal standard. Melting points were determined in open capillaries on an Optimelt MPA100 device (Stanford Research Systems, England) and were not corrected. The specific optical rotation was measured on an ADP 440 Polarimeter (Bellingham + Stanley Ltd., England). TLC was performed on Kieselgel 60 G/F_{254} plates (Merck, Germany) in the following chromatographic systems: (A), chloroform–methanol (9 : 1); (B) dioxane–water (9 : 1); (C), *n*-butanol–acetic acid–water (4 : 1 : 1); (D), *n*-butanol–acetic acid–water (3 : 1 : 1); (E), chloroform–methanol–water–acetic acid (8 : 10 : 2 : 3); (F), chloroform–methanol–water–acetic acid (15 : 10 : 2 : 3); (G), isopropanol–benzene–aqueous ammonia (10 : 3 : 3). The amine-containing compounds, the compounds with amide groups, the compounds with free carboxyl groups, and the aromatic-containing compounds were detected by the ninhydrin treatment, by keeping in iodine vapor, by the treatment with chlorine with the subsequent staining by *o*-tolidine, by the treatment with bromocresol green, and in UV-light, respectively.

An analytical HPLC of the dipeptides was carried out on a Wellchrom 2001 chromatographic system (KNAUER, Germany) equipped with a Disorb-130-C16T column C16T (4.6 × 150 mm, 7 μm) in a concentration gradient of acetonitrile in 0.5% TFA from 0 to 30%, within 20 min at a flow rate of 1 mL/min at 214 nm.

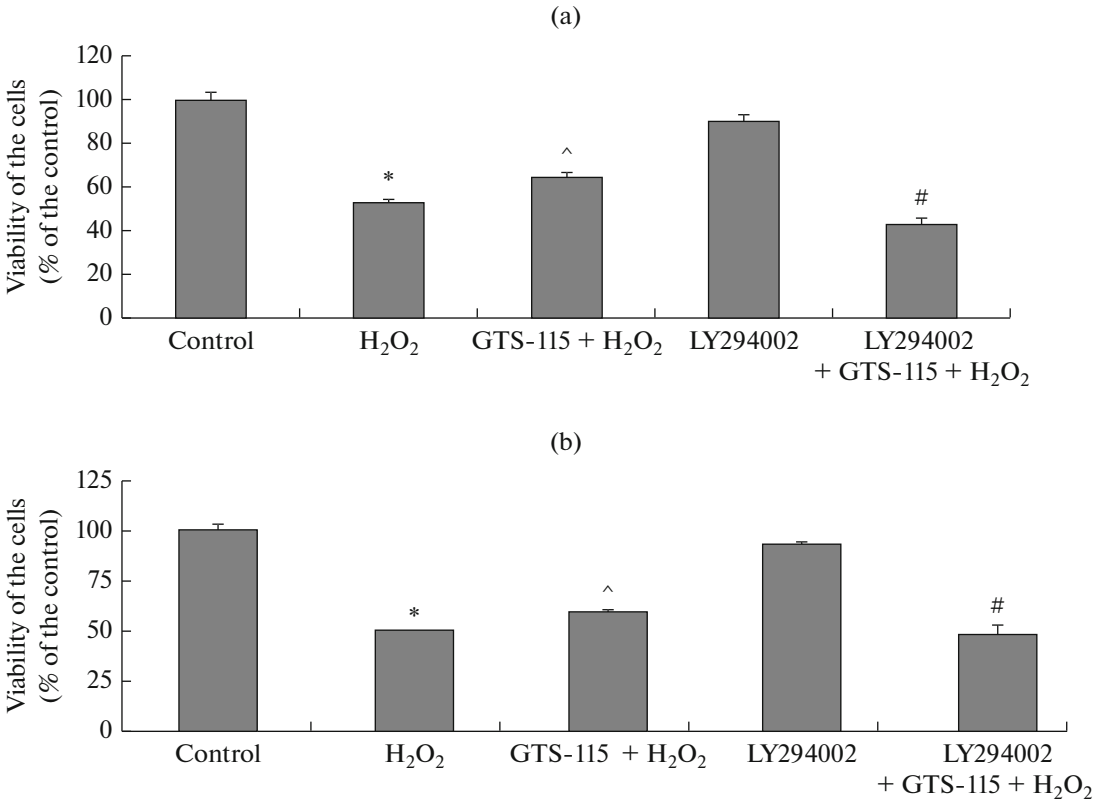

Fig. 3. The LY294002 inhibitor of phosphatidylinositol-3-kinase prevents the neuroprotective effect of the GTS-115 mimetic of the third loop of NGF on the model of the oxidative stress in the culture of the HT-22 hippocampal neurons. GTS-115 was introduced (a) 24 h before the hydrogen peroxide and (b) just after hydrogen peroxide. The data are presented as the mean deviations and the root-mean-square deviations. * $p < 0.05$ in comparison with the control (without H_2O_2 and GTS-115), ^ $p < 0.05$ in comparison with the damage (H_2O_2), #$p < 0.05$ in comparison with H_2O_2 + GTS-115 (the ruskal–Wallis criterion with the subsequent pairwise intergroup comparison with the use of the Dann-test).

Synthesis of the starting compounds

Z-Lys(Boc)-ONSu (I) was prepared according to a procedure [19] with a yield of 95%; R_f 0.90 (A) and R_f 0.83 (B); mp 97–99°C (isopropanol); $[\alpha]_D$ –16.0° (*c* 2, dioxane). The literature data [20]: mp 96–98°C (isopropanol–petroleum-ether); $[\alpha]_D$–16.1° (*c* 2, dioxane).

$CH_3COONSu$ was prepared by the procedure [6]. The yield 93%; R_f 0.40 (A) and R_f 0.75 (B); mp 103–105°C. The literature data [6]: R_f 0.41 (A) and R_f 0.75 (B); mp. 103–105°C. The ^{1}H NMR spectrum (DMSO-d_6): 2.34 (3 H, s, CH_3CO–), 2.80 (4 H, m, $-CH_2CH_2-$, –OSu).

Synthesis of 2 HCl · (HO-$(CH_2)_3$-CO-Lys-His-NH-)$_2$-$(CH_2)_6$ (GTS-115)

Z-Lys(Boc)-His-OMe (II). 2 HCl · H-His-OMe (30.2 g, 125 mmol) and TEA (35 mL, 250 mmol) were added to the solution of Z-Lys(Boc)-ONSu (**I**) (54.8 g, 115 mmol) in chloroform (250 mL). The reaction mixture was stirred at room temperature for 48 h, diluted with water (300 mL) and petroleum-ether (300 mL), and kept in a refrigerator (+4°C) for 12 h. The precipitate was filtered, washed with water (200 mL) and petroleum-ether (200 mL). The product was obtained as a white powder. The yield 52.6 g (86%); R_f 0.85 (F) and R_f 0.66 (D); mp 105–108°C, $[\alpha]_D$–6.3° (*c* 1; DMF); $[\alpha]_D$ –3.2° (*c* 1.05; methanol); ^{1}H NMR (DMSO-d_6): 1.18–1.60 (6 H, m, $C^{\gamma}H_2$ Lys, $C^{\delta}H_2$ Lys, $C^{\beta}H_2$ Lys), 1.37 (9 H, s, $-OC(CH_3)_3$), 2.87–2.92 (4 H, m, $C^{\beta}H_2$ His, $C^{\varepsilon}H_2$ Lys), 3.57 (3 H, s, $-OCH_3$), 3.98 (1 H, m, $C^{\alpha}H$ Lys), 4.48 (1 H, m, $C^{\alpha}H$ His), 5.02 (2 H, m, $C_6H_5C\underline{H}_2O$–), 6.76 (1 H, t, *J* 5.4, $N^{\varepsilon}H$ Lys), 6.84 (1 H, s, $C^4\underline{H}$-imidazole ring of His), 7.20–7.29 (6 H, m, 2 $C_6\underline{H}_5CH_2O$–, NH Lys), 7.56 (2 H, s, $C^2\underline{H}$-imidazole ring of His), 8.33 (1 H, d, *J* 8.5, NH His).

Z-Lys(Boc)-His-N_2H_3 (III). Hydrazine hydrate (50 mL) was added to the solution of ester (**II**) (51.7 g, 93 mmol) in the mixture of DMF (150 mL) and BuOH (150 mL). The reaction mixture was kept 12 h with the TLC-monitoring. After the starting compound disappeared, methanol (100 mL) and water (150 mL) were added, and the reaction mixture was

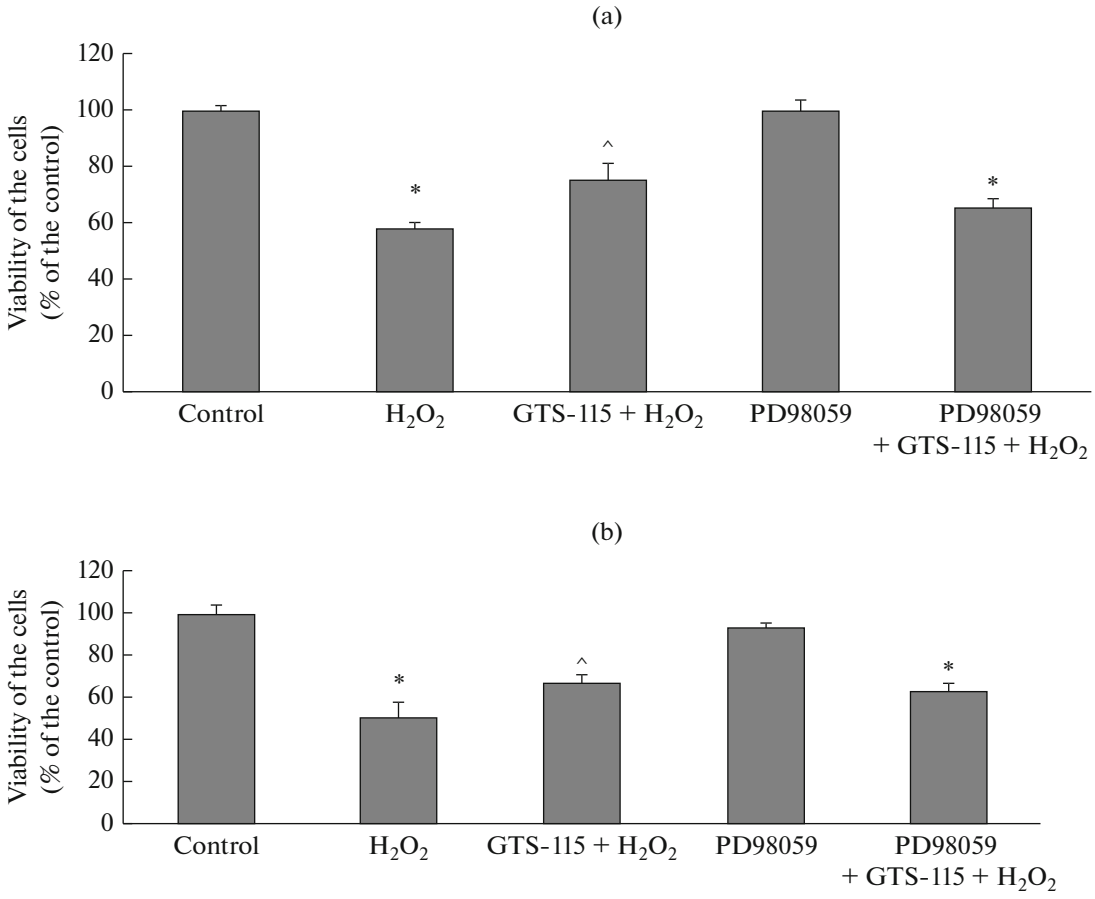

Fig. 4. The PD98059 specific inhibitor of the MEK1 and MEK2 mitogen-activated kinases partially prevents a development of the neuroprotective effect of the GTS-115 mimetic of the third loop of NGF on the model of the oxidative stress in the culture of the HT-22 hippocampal neurons. GTS-115 is introduced (a) 24 h before hydrogen peroxide and after hydrogen peroxide. The data are presented as mean deviations and root-mean-square deviations. * $p < 0.05$ in comparison with the control, ^ $p < 0.05$ in comparison with the H_2O_2 damage, # $p < 0.05$ in comparison with H_2O_2+GTS-115 (the Kruskal–Wallis criterion with the subsequent pairwise intergroup comparison with the use of the Dann-test).

kept at −20°C for 12 h. The precipitate was filtered, washed with a cool aqueous methanol, and dried in air. The yield of hydrazide (**III**) was 49.6 g (96%); R_f 0.53 (D), 0.92 (E), 0.57 (F); mp 146–149°C, $[\alpha]_D$ −8.7° (*c* 1.05, DMF); ^{1}H NMR (DMSO-d_6): 1.15–1.41 (4 H, m, $C^{\gamma}H_2$ Lys, $C^{\delta}H_2$ Lys), 1.37 (9 H, s, $-OC(CH_3)_3$), 1.44–1.61 (2 H, m, $C^{\beta}H_2$ Lys), 2.70–2.95 (4 H, m, $C^{\beta}H_2$ His, $C^{\varepsilon}H_2$ Lys), 3.94 (1 H, m, $C^{\alpha}H$ Lys), 4.43 (1 H, m, $C^{\alpha}H$ His), 5.06 and 5.01 (2 H, two doublets, *J* 12.8, $C_6H_5C\underline{H}_2O-$), 6.78 (2 H, broadened s, 2 $N^{\varepsilon}H$ Lys, 2 $C^2\underline{H}$-imidazole ring of His), 7.25–7.29 (5 H, m, $C_6\underline{H}_5CH_2O-$), 7.45 (2 H, d, *J* 7.6, NH Lys), 7.49 (1 H, s, $C^4\underline{H}$-imidazole ring of His), 8.07 (1 H, d, *J* 7.9, NH His). 9.04 (1 H, s, $N\underline{H}-NH_2$).

(Z-Lys(Boc)-His-NH-)$_2$(CH$_2$)$_6$ (IV). 4 M HCl (65 mL) in dioxane and BuONO (10.5 mL, 88 mmol) were added to the cooled (−20°C) solution of hydrazide (**III**) (46.0 g, 86.4 mmol) in DMF (300 mL). The reaction mixture was kept at −20 to −30°C for 3 min, and TEA (36 mL, 260 mmol) and, then, the solution of hexamethylenediamine (4.7 g, 40.5 mmol) in DMF (40 mL) were added. The reaction mixture was kept at room temperature for 12 h, diluted with water (1.5 L), and the precipitate was allowed to form for 12 h. The precipitate was filtered, dissolved in methanol (300 mL), diluted with water (150 mL), and cooled to −20°C in a freezing chamber. The precipitate was filtered at room temperature, washed with aqueous methanol (300 mL), and dried in air. Product (**IV**) was obtained as white crystals. The yield 38.1 g (79%); R_f 0.60 (D), 0.80 (F); mp 135–138°C; $[\alpha]_D$ −11.1° (*c* 1.05; DMF), $[\alpha]_D$−16.6° (*c* 1.05; methanol); ^{1}H NMR (DMSO-d_6): 0.99–1.13 (8 H, m, $-NHCH_2(C\underline{H}_2)_4CH_2NH-$,), 1.15–1.44 (8 H, m, 2 $C^{\gamma}H_2$ Lys, 2 $C^{\delta}H_2$ Lys), 1.44–1.68 (4 H, m, 2 $C^{\beta}H_2$ Lys), 1.37 (18 H, s, 2 $-OC(CH_3)_3$), 2.76–2.92 (4 H, m, 2 $C^{\beta}H_2$ His, 2 $C^{\varepsilon}H_2$ Lys), 2.92–3.05 (4 H, m, $-NHC\underline{H}_2(CH_2)_4C\underline{H}_2NH-$), 3.91 (2 H, m, 2 $C^{\alpha}H$ Lys), 4.41 (2 H, m, 2 $C^{\alpha}H$ His), 5.03 (4 H,

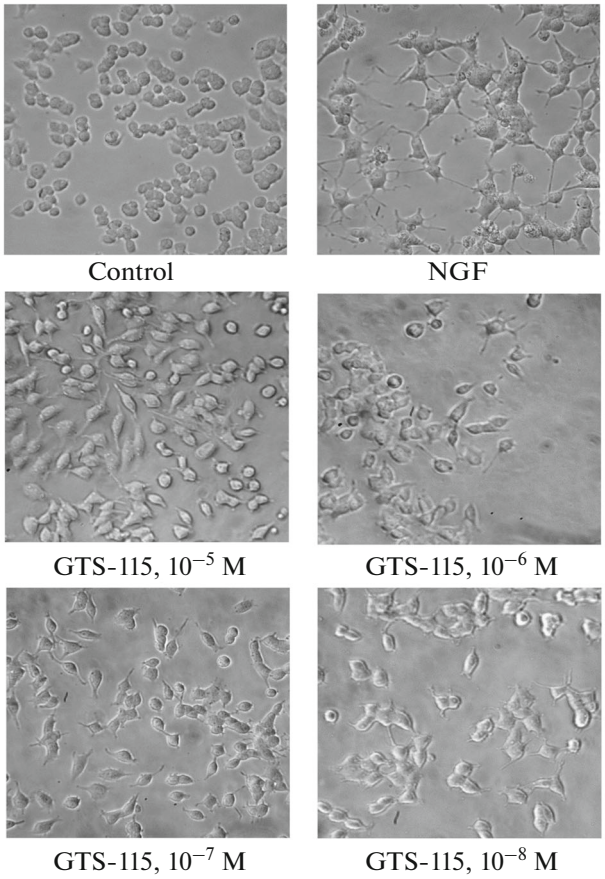

Fig. 5. The GTS-115 mimetic of the third loop of NGF exhibits the differentiating activity towards the pheochromocytoma cells of the PC12 line.

m, 2 $C_6H_5C\underline{H}_2O$–), 6.75 (2 H, t, *J* 5.7, 2 $N^{\varepsilon}H$ Lys), 6.78 (2 H, s, $C^4\underline{H}$-imidazole ring of His), 7.20–7.41 (10 H, m, 2 $C_6\underline{H}_5CH_2O$–), 7.49 (2 H, s, $C^2\underline{H}$-imidazole ring of His), 7.53–7.65 (4 H, d, 2 NH Lys, t, *J* 5.1, $-N\underline{H}(CH_2)_6N\underline{H}$–), 8.24 (2 H, d, *J* 8.5, 2 NH His).

(H-Lys(Boc)-His-NH-)$_2$(CH$_2$)$_6$ (V). 10% Pd/C (3 g) was added to the solution of derivative (**IV**) (33.0 g, 29.5 mmol) in methanol (500 mL). The reaction mixture was stirred for 6–12 h in the hydrogen atmosphere to a complete disappearance of the starting compound (TLC monitoring). The catalyst was filtered off after completion of hydrogenolysis. The filtrate was evaporated, dissolved in isopropanol, and evaporated again. The solid residue was triturated with ether, filtered, and dried in vacuum (15 mmHg). Diamide (**V**) was obtained as a white powder. The yield was 23.5 g (94%); R_f 0.10 (D); mp 105–106°C; $[\alpha]_D$ –0.9° (*c* 1.05, methanol); ^{1}H NMR (DMSO-d_6): 1.00–1.60 (20 H, m, $-NHCH_2C\underline{H}_2(C\underline{H}_2)_2C\underline{H}_2CH_2NH$–, 2 $C^{\gamma}H_2$ Lys, 2 $C^{\delta}H_2$ Lys, 2 $C^{\beta}H_2$ Lys), 1.37 (18 H, s, 2 $-OC(CH_3)_3$), 2.86 (4 H, m, 2 $C^{\beta}H_2$ His, 2 $C^{\varepsilon}H_2$ Lys), 2.93 (4 H, m, $-NHC\underline{H}_2(CH_2)_4C\underline{H}_2NH$–), 3.91 (2 H, m, 2 $C^{\alpha}H$ Lys), 4.41 (2 H, m, 2 $C^{\alpha}H$ His), 6.75 (2 H, t, *J* 5.7, 2 $N^{\varepsilon}H$ Lys), 6.78 (2 H, s, $C^4\underline{H}$-imidazole ring of His), 7.48 (2 H, s, $C^2\underline{H}$-imidazole ring of His), 7.58 (2 H, d,

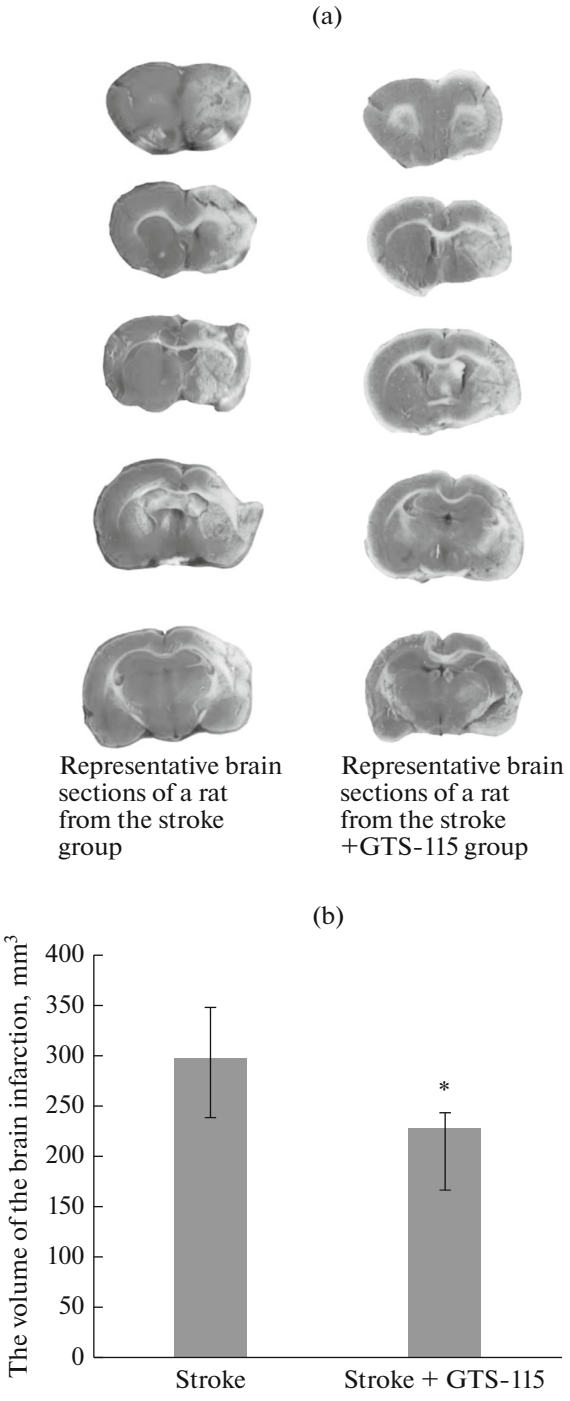

Fig. 6. (a) Representative TTC-stained brain sections. (b) GTS-115 decreases the volume of the brain infarction according to the results of the morphometry of the TTC-stained sections on the 8th day after the transient occlusion of the medial cerebral artery. The data are presented as medians and interquartile intervals. * $p < 0.05$ relatively to the stroke group (the Mann–Whitney U-test).

Comparison of the biochemical and pharmacological properties of the dipeptide mimetics of the first, third, and fourth loops of the NGF neurotrophine

Properties	Mimetic of the third loop, GTS-115	Mimetic of the first loop [9] GK-6	Mimetic of the fourth loop [9] GK-2	NGF
Activation TrkA	+	+	+	+
Activation PI3K/AKT	+	+	+	+
Activation MAPK/ERK	+	+	0	+
Neuroprotective activity	+	+	+	+
Differentiating activity	+	+	0	+
Hyperalgesia	+	+	0	+
Effect on the body weight	0	0	0	+

+ is a positive effect, 0 is a negative effect.

2 NH Lys), 7.61 (2 H, t, *J* 5.1, $-N\underline{H}(CH_2)_6N\underline{H}-$), 8.24 (2 H, d, *J* 8.5, 2 NH His).

(HO-$(CH_2)_3$-CO-Lys(Boc)-His-NH-)$_2(CH_2)_6$(VI). The solution of diamide (**V**) (0.50 g, 0.60 mmol) in butyrolactone (6 mL) was heated to 50–60°C, kept at this temperature for 4 h, and stirred at room temperature for 12 h. The precipitate was carefully triturated with ether (4 × 10 mL) with decantation. The residue was dried in vacuum (15 mmHg) over $CaCl_2$ and crystallized from hot acetone. The yield of amorphous white powder was 0.56 g (93%); R_f 0.28 (C), 0.53 (D); mp 174–179°C with a decomposition; $[\alpha]_D$–20.8° (*c* 1.05, methanol); ^{1}H NMR (DMSO-d_6): 1.03–1.36 (16 H, m, $-NHCH_2C\underline{H}_2(C\underline{H}_2)_2C\underline{H}_2CH_2NH-$, 2 C$^\gamma$H$_2$ Lys, and 2 C$^\delta$H$_2$ Lys), 1.37 (18 H, s, 2 $-OC(CH_3)_3$), 1.58 (4 H, m, 2 C$^\beta$H$_2$ Lys), 1.64 (4 H, t, *J* 7.0, 2 C^{2}H$_2$ GHB), 2.24 (4 H, t, *J* 7.0, 2 C^{1}H$_2$ GHB), 2.73 (4 H, m,), 2.86 (4 H, m, 2 C$^\beta$H$_2$ His and 2 C$^\varepsilon$H$_2$ Lys), 2.96 (4 H, m, $-NHC\underline{H}_2(CH_2)_4C\underline{H}_2NH-$), 3.40 (4 H, t, *J* 7.0, 2 C^{3}H$_2$ GHB), 4.02 (2 H, m, 2 C$^\alpha$H Lys), 4.35 (2 H, m, 2 C$^\alpha$H His), 4.56 (2 H, broadened s, 2 OH GHB), 6.76 (2 H, t, *J* 5.7, 2 N$^\varepsilon$H Lys), 6.76 (2 H, s, C$^4\underline{H}$-imidazole ring of His), 7.46 (2 H, t, *J* 5.1, $-N\underline{H}(CH_2)_6N\underline{H}-$), 8.17 (2 H, d, *J* 7.0, 2 NH Lys), 8.26 (2 H, d, *J* 8.5, 2 NH His), 7.54 (2 H, s, C$^2\underline{H}$-imidazole ring of His), 11.81 (2 H, broadened s, 2 N$\underline{H}$-imidazole ring of His); ^{1}H NMR (DMSO-d_6-CF_3COOH): 1.03–1.42 (16 H, m, $-NHCH_2C\underline{H}_2(C\underline{H}_2)_2C\underline{H}_2CH_2NH-$, 2 C$^\gamma$H$_2$ Lys, and 2 C$^\delta$H$_2$ Lys), 1.36 (18 H, s, 2 $-OC(CH_3)_3$), 1.42–1.56 (4 H, m, 2 C$^\beta$H$_2$ Lys), 1.63 (4 H, t, *J* 7.0, 2 C^{2}H$_2$ GHB), 2.17 (4 H, t, *J* 7.0, 2 C^{1}H$_2$ GHB), 2.86 (2 H, m, 2 C$^\varepsilon$H$_2$ Lys), 2.83–3.13 (8 H, m, 2 C$^\beta$H$_2$ His and $-NHC\underline{H}_2(CH_2)_4C\underline{H}_2NH-$), 3.38 (4 H, t, *J* 7.0, 2 C^{3}H$_2$ GHB), 4.04 (2 H, m, 2 C$^\alpha$H Lys), 4.50 (2 H, m, 2 C$^\alpha$H His), 6.74 (2 H, t, *J* 5.7, 2 N$^\varepsilon$H Lys), 7.32 (2 H, s, C$^4\underline{H}$-imidazole ring of His), 7.79 (2 H, t, *J* 5.0, $-N\underline{H}(CH_2)_6N\underline{H}-$), 8.03 (2 H, d, *J* 8.0, 2 NH Lys), 8.13 (2 H, d, *J* 8.0, 2 NH His), 8.97 (2 H, s, C$^2\underline{H}$-imidazole ring of His), 14.10 (2 H, broadened s, 2 N$\underline{H}$-imidazole ring of His); ^{13}C NMR (DMSO-d_6)*:* 26.29 and 23.28, 28.77, 29.77, 29.25, 28.90, 31.20, 31.40, 32.46, 39.73, 39.00, 53.30, 54.20, 60.85, 77.84, 135.20, 156.00, 174.00, 173.90, 172.00.

2HCl · (HO-$(CH_2)_3$-CO-Lys-His-NH-)$_2(CH_2)_6$ (GTS-115). 4 M HCl in dioxane (5 mL) was added to the suspension of (HO-$(CH_2)_3$-CO-Lys(Boc)-His-NH-)$_2(CH_2)_6$ (0.30 g, 0.29 mmol) in dioxane (10 mL) on cooling to 5 to 10°C and stirring. The reaction mixture was stirred for 2.5 h, and the solvent was decanted. The crystalline residue was triturated over dioxane (2 × 15 mL) and, then, over ether (3 × 15 mL) with a decantation. The crystals were filtered and dried in vacuum (15 mmHg) over KOH. The yield of the solid white product was 0.23 g (90%); R_f 0.05 (E); HPLC: τ = 8.3 min; mp 120°C with decomposition; $[\alpha]_D$–23.3° (*c* 1.05, water); ^{1}H NMR (D_2O): 1.10–1.18 (4 H, m, $-NHCH_2CH_2(C\underline{H}_2)_2C\ H_2CH_2NH-$), 1.22–1.43 (8 H, m, $-NHCH_2C\underline{H}_2(CH_2)_2C\underline{H}_2CH_2NH-$ and 2 C$^\gamma$H$_2$ Lys), 1.53–1.68 (8 H, m, 2 C$^\beta$H$_2$ Lys and 2 C$^\delta$H$_2$ Lys), 1.74 (4 H, t, *J* 6.8, 2 C^{2}H$_2$ GHB), 2.28 (4 H, t, *J* 7.5, 2 C^{1}H$_2$ GHB), 2.91 (2 H, t, *J* 7.5, 2 C$^\varepsilon$H$_2$ Lys), 3.02–3.24 (8 H, m, 2 C$^\beta$H$_2$ His and $-NHC\underline{H}_2(CH_2)_4C\underline{H}_2NH-$), 3.52 (4 H, t, *J* 6.8, 2 C^{3}H$_2$ GHB), 4.14 (2 H, m, 2 C$^\alpha$H Lys), 4.56 (2 H, m, 2 C$^\alpha$H His), 7.25 (2 H, s, C$^4\underline{H}$-imidazole ring of His), 7.97 (2 H, t, *J* 5.1, $-N\underline{H}(CH_2)_6N\underline{H}-$), 8.20 (2 H, d, *J* 7.0, 2 NH Lys), 8.49 (2 H, d, *J* 8.5, 2 NH His), 8.59 (2 H, s, C$^2\underline{H}$-imidazole ring of His); ^{1}NMR (DMSO-d_6): 1.15–1.43 (12 H, m, $-NHCH_2-(C\underline{H}_2)_4CH_2NH-$ and 2 C$^\gamma$H$_2$ Lys), 1.47–1.60 (8 H, m, 2 C$^\beta$H$_2$ Lys and 2 C$^\delta$H$_2$ Lys), 1.64 (4 H, t, *J* 6.8, 2 C^{2}H$_2$ GHB), 2.20 (4 H, t, *J* 7.5, 2 C^{1}H$_2$ GHB), 2.73 (2 H, m, 2 C$^\varepsilon$H$_2$ Lys), 2.95–3.18 (8 H, m, 2 C$^\beta$H$_2$ His and $-NHC\underline{H}_2(CH_2)_4C\underline{H}_2NH-$), 3.38 (4 H, t, *J* 6.8, 2 C^{3}H$_2$ GHB), 4.09 (2 H, dd, *J* 6.0, *J* 7.3, 2 C$^\alpha$H Lys), 4.53 (2 H, dd, *J* 6.1, *J* 9.2, 2 C$^\alpha$H His), 7.37 (2 H, s, C$^4\underline{H}$-imidazole ring of His), 7.96 (2 H, t, *J* 5.1, $-N\underline{H}(CH_2)_6N\underline{H}-$),

8.03 (6 H, broadened s, 2 $^{+}N^{\varepsilon}\underline{H}_3$ Lys), 8.20 (2 H, d, *J* 7.0, 2 NH Lys), 8.24 (2 H, d *J* 8.5, 2 NH His), 9.03 (2 H, s, $C^2\underline{H}$-imidazole ring of His), 14.47 (2 H, broadened s, 2 N$\underline{H}$-imidazole ring of His).

Synthesis of 2HCl · (CH_3CO-Lys-His-NH-)$_2(CH_2)_6$ (GTS-113)

(CH_3CO-Lys(Boc)-His-NH-)$_2(CH_2)_6$. $CH_3COONSu$ (0.190 g, 1.22 mmol) was added to the solution of diamide **(V)** (0.425 g, 0.50 mmol) in DMF (15 mL) on stirring and cooling to 5°C. The reaction mixture was kept at this temperature for 1 h and at room temperature for 12 h and evaporated. The residue was triturated with ether, decanted, crystallized from hot acetone, and dried in vacuum (15 mmHg) over $CaCl_2$. The yield was 0.37 g (80%); R_f 0.57 (H); mp 190°C with decomposition; $[\alpha]_D$–18.1° (*c* 1, methanol), $[\alpha]_D$–12.2° (*c* 1; methanol); ^{1}H NMR (DMSO-d_6): 0.95–1.12 (4 H, m, –NH$(CH_2)_2(C\underline{H}_2)_2(CH_2)_2$NH–), 1.20–1.32 (12 H, m, –NHCH$_2C\underline{H}_2(CH_2)_2C\underline{H}_2CH_2$NH– and 2 $C^{\gamma}H_2$ Lys, 2 $C^{\delta}H_2$ Lys), 1.36 (18 H, s, 2 –OC$(CH_3)_3$), 1.49–1.58 (4 H, m, 2 $C^{\beta}H_2$ Lys), 1.90 (6 H, s, 2 –OCCH_3), 2.80–2.98 (8 H, m, 2 $C^{\varepsilon}H_2$ Lys and 2 $C^{\beta}H_2$ His, –NH-$C\underline{H}_2(CH_2)_4C\underline{H}_2$NH–), 4.00 (2 H, m, 2 C^{α}H Lys), 4.33 (2 H, m, 2 C^{α}H His), 6.76 (2 H, t, *J* 5.7, 2 N^{ε}H Lys), 6.76 (2 H, s, $C^4\underline{H}$-imidazole ring of His), 7.43 (2 H, broadened t, –N$\underline{H}(CH_2)_6$N$\underline{H}$–), 7.55 (2 H, s, $C^2\underline{H}$-imidazole ring of His), 8.24 (2 H, d, *J* 7.2, 2 NH Lys), 8.34 (2 H, d, *J* 6.2, 2 NH His), 11.63 (2 H, broadened s, 2 N$\underline{H}$-imidazole ring of His).

2HCl · (CH_3CO-Lys-His-NH-)$_2(CH_2)_6$. 4 M HCl in dioxane (15 mL) was added to the suspension of derivative **(VII)** (0.45 g, 0.48 mmol) in dioxane (15 mL). The reaction mixture was stirred for 2 h, and the solvent was decanted. The residue was triturated with ether (3 × 30 mL). The obtained crystals were filtered and dried in vacuum (15 mmHg) over KOH. The yield of the hygroscopic lightly cream-colored product was 0.36 g (92%); $[\alpha]_D$ – 11.1° (*c* 1, water); ^{1}H NMR (DMSO-d_6): 1.20–1.28 (4 H, m, –NH$(CH_2)_2(C\underline{H}_2)_2(CH_2)_2$NH– and 4 H, m, 2 $C^{\gamma}H_2$ Lys), 1.36 (4 H, m, –NHCH$_2C\underline{H}_2(CH_2)_2$-$C\underline{H}_2CH_2$NH–), 1.54 (8 H, m, 2 $C^{\beta}H_2$ and 2 $C^{\delta}H_2$ Lys), 1.87 (6 H, s, 2 -OCCH_3), 2.95–3.16 (12 H, m, 2 $C^{\varepsilon}H_2$ Lys, 2 $C^{\beta}H_2$ His and –NHC$\underline{H}_2(CH_2)_4C\underline{H}_2$NH–), 4.08 (2 H, m, 2 C^{α}H Lys), 4.52 (2 H, m, 2 C^{α}H His), 7.36 (2 H, s, $C^4\underline{H}$-imidazole ring of His), 7.99 (2 H, t, *J* 5.1, –N$\underline{H}(CH_2)_6$N$\underline{H}$–), 8.06 (6 H, broadened s, 2 $^{+}N^{\varepsilon}\underline{H}_3$ Lys), 8.27 (2 H, d, *J* 7.0, 2 NH Lys), 8.32 (2 H, d, *J* 8.5, 2 NH His), 9.03 (2 H, s, $C^2\underline{H}$-imidazole ring of His), 14.49 (2 H, broadened s, 2 N$\underline{H}$-imidazole ring of His).

Studies of the Biological Activity In Vitro

The neuroprotective activity of the compounds was examined on *the model of the oxidative stress* [10]. The mouse hippocampal immortalized cells of the HT-22 line were seeded in the poly-Lys-treated 96-well plates (BD Biosciences, San Jose, United States, 5 μg/cm^2) with a density of 3500 cells per one well in the DMEM medium (Thermo Fisher Scientific, Waltham, United States) containing 5% embryonic calf serum (Gibco Life Technologies, New York, United States) and 2 mM L-glutamine (ICN, Eschwege, Germany) and incubated at 37°C in the atmosphere of 5% CO_2 to the formation of a monolayer. The oxidative stress was modeled by the incubation of the cells with H_2O_2 in the final concentration of 1.5 mM C in an atmosphere of 5% CO_2 at 37°C. Then, the medium was replaced by the normal one, hydrogen peroxide was washed out, and, four hours later, the viability of the cells was determined with the use of bromide of 3-(4,5-dimethylthiazole-2-yl)-2,5-diphenyl tetrazolium (the MTT-test) (Sigma, St. Louis, United States) [21]. The optical absorption was measured on a "Multiscan EX" spectrophotometer (Thermo Fisher Scientific, Waltham, United States) at 600 nm. The peptides were introduced 24 h before the damage or just after the washing from H_2O_2 in an aqueous solution in the range of the final concentrations from 10^{-5} to 10^{-8}M.

The activity of resistance to the oxidative stress was calculated by the equation: $A(\%) = (D_{exp} - D_{H_2O_2})/(D_{cont} - D_{H_2O_2}) \times 100\%$, where D_{exp}, and D_{cont} were the optic absorptions of the experimental solution and the solutions of the active (with H_2O_2) and the passive (without H_2O_2) controls, respectively.

Influence of GTS-115 on phosphorylation of the TrkA receptor and Akt1/2/3 and ERK1/2 kinases. Contents of pTrkA, TrkA, pAkt1/2/3, Akt1/2/3, pERK1/2, and ERK1/2 were determined by Western-blot analysis. The cells were seeded on Petri dishes with a density of 20 000 cells/cm^2 and incubated for 2 days. The aqueous solution of GTS-115 (10^{-6} M) was added in the culture medium and 30, 60, and 180 min later, and the dishes from the culture medium were washed with the PBS buffer (Sigma, St. Louis, United States). The lysing buffer (Bio-Rad, Hercules, United States; 50 mM Tris-HCl, 5mM EDTA, 1 mM DTT, and 1% Triton X-100) was added at pH 7.5 and 4°C. The cells were lysed for 5 min on ice, scraped off, placed in a centrifugal tube 1.5 mL in volume, and centrifuged for 10 min at 13 000 rpm at 4°C. The protein concentration was determined by the Folin–Lowry method [22]. The proteins were fractionated by electrophoresis in 10% PAAG (Bio-Rad, Hercules, United States) in the presence of sodium dodecyl sulfate [23]. The proteins were transferred from PAAG onto a PVDF membrane (Bio-Rad, Hercules, United States) by electroelution within 45 min. The Western-

blots were preincubated in the TBS buffer with 1% Tween-20 and 5% (weight/volume) fat-free milk (buffer A) overnight, incubated in the presence of the mouse monoclonal antibodies against the phosphorylated and nonphosphorylated forms of the tyrosine kinase A (pTrkA, in a dilution of 1 : 1000 for 1 h, against the rabbit polyclonal antibodies to the phosphorylated and nonphosphorylated forms of Akt/2/3 and pAkt/2/3 kinases (Santa Cruz Biotechnology, Santa Cruz, United States), against phosphorylated (the rabbit polyclonal antibodies) and nonphosphorylated (the mouse monoclonal antibodies) forms of ERK1/2 and pERK1/2 (Santa Cruz Biotechnology, Santa Cruz, United States) in a dilution of 1 : 1000 for 1 h, washed with buffer A, and incubated in the presence of the second goat antibodies (Santa Cruz Biotechnology, Santa Cruz, United States) conjugated with the horseradish peroxidase (the dilution was 1 : 2000) for 1 h. The proteins were detected after the washing from the second antibodies with buffer A by the reaction with the ECL-reagents (Santa Cruz Biotechnology, Santa Cruz, United States) using the Alliance UVITEC gel-documenting system (the United Kingdom). A densitometry of blots was performed using the GIMP2 program. Beta-actin was used as a loading control protein (see Fig. 2).

The differentiating activity of GTS-115. The PC12 nondifferentiated cells were seeded with a density of 3500 cells/well in the DMEM medium (Thermo Fisher Scientific, Waltham, United States) containing 1% embryonic calf serum (Gibco Life Technologies, New York, United States) and 2 mM *L*-glutamine (ICN, Eschwege, Germany) in an atmosphere of 5% CO_2 at 37°C. NGF (100 ng/mL, positive control) or GTS-115 in the concentration range from 10^{-5} to 10^{-8} M were added to the culture medium at the seeding moment. Further, GTS-115 and NGF were added to the medium every 48 h during 6 days [24]. The cells with the processes whose length was longer than the diameter of the cell body were considered to be differentiated.

Inhibitory analysis. The LY294002 inhibitor of phosphatidylinositol-3-kinase (Sigma, St. Louis, United States) [25] and the PD98059 specific inhibitor of the MEK1and MEK2 mitogen-activated protein kinases (Sigma, St. Louis, United States) [26] were used for the studies of the involvement of the two main signal pathways which were activated by the NGF binding to its specific tyrosine-kinase TrkA receptor in the neuroprotective effect of the GTS-115 dimeric dipeptide mimetic of the third NGF loop.

The investigation was performed on the model of the oxidative stress as it was described above with the use of the hippocampal neurons of the HT-22 line. The specific inhibitors were applied as their solutions in 10% aqueous 2-hydroxypropyl-β-cyclodextrin (AppliChem, Darmstadt, Germany) and introduced in their final concentrations of 100 μM (LY294002) and 50 μM (PD98059) 30 min before GTS-115 which were added 24 h before the injury. In another variation, the inhibitors were added just after the washing from hydrogen peroxide, and GTS-115 was added 30 min after the inhibitors. The concentrations and the time of the inhibitor addition were chosen according to [27]. GTS-115 was introduced in the highest neuroprotective concentration in vitro (10^{-6} M).

Studies of the Biological Activity In Vivo

The neuroprotective properties of GTS-115 were studied on the model of ischemic stroke induced by the occlusion of the medial cerebral artery in rats. The experiments were performed on outbred male rats (230–290 g of body weight at the beginning of the experiment). The ischemic stroke was modeled by an intravascular blockage of the medial cerebral artery by a nylon thread [13]. The blood flow was blocked for one hour, and the thread was removed. Sham-operated animals were subjected to the same procedures as the operated rats except for the vessel cutting and the thread introduction and were used as a control during the examination of the neurological state. The solution of GTS-115 in distilled water at a dose of 1 mg/kg intraperitoneally or distilled water alone were administered to the animals 4 h after the operation and, further, one time a day during the next six days (seven injections in all). The neurological deficit was evaluated in the limb-placing test [14, 15] 3 and 7 days after the operation. The animals were decapitated just after the last test, their brains were isolated and frozen at –20°C for 10 min. The frontal sections (1.7 mm) of the brain were made and stained in the 2% solution of 2,3,5-triphenyltetrazolium chloride (TTC) in the PBS buffer at 37°C for 20 min. The morphometric analysis of the images that were scanned on both sides was carried out using the free ImageJ program (National Institute of Health). The infarction volume was determined as a sum of the injury volumes in every section. The experimental groups were: "the sham-operated" ($n = 6$), "the stroke" ($n = 9$), and "the stroke + GTS-115" ($n = 7$).

The influence of GTS-115 on the pain sensitivity of the rats was determined in the hot plate test [18]. The experiments were performed on outbred male rats with the body weight of 240–260 g. The 2–3-min handling procedure was carried out for each animal during 3–4 days before the experiments in order to decrease the stress level during the experiment. The rats were placed in an experimental room one day before the experiment. The tests were held in the time interval from 17.00 to 20.00.

The control and experimental animals were placed on a working place of an "Ugo Basile" analgesiometer. It looked like a metallic disc which was heated to the desired temperature (54 ± 0.1°C) and thermostatically controlled. A plexiglass cylinder 35 mm in height open at the upper end was positioned on the disc. Therefore, a rat

was placed inside the cylinder at its bottom which was the heated disc (the hot plate).

The animals were divided into three groups (10 animals in each). The control group was injected with distilled water. GTS-115 at doses of 0.1 and 1.0 mg/kg was administered to the other two groups. The solvent and the examined compound were introduced intraperitoneally.

The reaction time of a rat to the thermic stimulus was measured after its placement on the hot plate. The maximum permissible reaction time was 20 s. The starting average parameters of the pain thresholds before the administration of the substances were determined based on four measurements at the 10-min intervals for every animal. The obtained average values of the latent period of the pain reaction were taken to be 100%. The effects were evaluated 24 h after the administration of the substance according to the data on the hyperalgesic effect of NGF [28].

Evaluation of a possible GTS-115 effect on the body weight was performed at the GTS-115 daily intraperitoneal administration to outbred male rats at a dose of 1 mg/kg for 14 days. The animals were divided into two groups (10 animals in each). The experimental and control groups got GTS-115 and distilled water, respectively, and were subjected to daily weighing.

Statistical analysis. The Mann–Whitney U-criterion was used for the comparison of the two groups. The one-factor dispersion Kruskal–Wallis analysis with the subsequent Dann post-test or the ANOVA one-factor dispersion analysis were applied to a comparison of three and more groups.

ACKNOWLEDGMENTS

This study was partially supported by the Russian Scientific Foundation (project no. 14-15-00596).

REFERENCES

1. Levi-Montalcini, R., *Science*, 1987, vol. 237, pp. 1154–1162.
2. Aloe, L., Rocco, M.L., Bianchi, P., and Manni, L., *J. Transl. Med.*, 2012, vol. 10, no. 11, pp. 239–252.
3. Kaplan, D.R. and Miller, F.D., *Curr. Opin. Neurobiol.*, 2000, vol. 10, no. 3, pp. 381–391.
4. Obata, K. and Noguchi, K., *Life Sci.*, 2004, vol. 74, no. 21, pp. 2643–5263.
5. Gudasheva, T.A., Antipova, T.A., and Seredenin, S.B., *Dokl. Biochem. Biophys.*, 2010, vol. 434, pp. 262–265.
6. Seredenin, S.B. and Gudasheva, T.A., Dipeptide mimetics of neurotrophins NGF and BDNF, RF Patent no. 2410392, *Byul. Izobret.*, 2011, no. 3.
7. Gudasheva, T.A., Povarnina, P.Yu., Antipova, T.A., and Seredenin, S.B., *Neurosci. Med.*, 2014, vol. 5, no. 2, pp. 101–108.
8. Seredenin, S.B. and Gudasheva, T.A., *Zh. Nevrol. Psikhiatr. im. S.S. Korsakova*, 2015, vol. 115, no. 6, pp. 63–70.
9. Gudasheva, T.A., Povarnina, P.Y., Antipova, T.A., Firsova, Y.N., Konstantinopolsky, M.A., and Seredenin, S.B., *J. Biomed. Sci.*, 2015, vol. 22, p. 106.
10. Jackson, G.R., Werrbach-Perez, K., Ezell, E.L., Post, J.F., and Perez-Polo, J.R., *Brain Res.*, 1992, vol. 592, nos. 1–2, pp. 239–248.
11. Virdee, K. and Tolkovsky, A.M., *J. Neurochem.*, 1996, vol. 67, no. 5, pp. 1801–1805.
12. Chang, J.H., Mellon, E., Schanen, N.C., and Twiss, J.L., *J. Biol. Chem.*, 2003, vol. 278, no. 44, pp. 42877–42885.
13. Longa, E.Z., Weinstein, P.R., Carlson, S., and Cummins, R., S*t*roke, 1989, vol. 20, no. 1, pp. 84–91.
14. De Ryck, M., Van Reempts, J., Borgers, M., Wauquier, A., and Janssen, P.A., *Stroke*, 1989, vol. 20, no. 10, pp. 1383–1390.
15. Jolkkonen, J., Puurunen, K., Rantakomi, S., Harkonen, A., Haapalinna, A., and Sivenius, J., *Eur. J. Pharmacol.*, 2000, vol. 400, nos. 2–3, pp. 211–219.
16. Hathway, G.J. and Fitzgerald, M., *J. Pain*, 2006, vol. 7, pp. 57–61.
17. Taglialatela, G., Foreman, P.J., and Perez-Polo, J.R., *Int. J. Dev. Neurosci.*, 1997, vol. 15, no. 6, pp. 703–710.
18. Khan, S.A., Chatterjee, S.S., and Kumar, V., *Life Sci.*, 2016, vol. 148, pp. 53–62.
19. Tarasyuk, A.V., Pomogaibo, S.V., Kurilov, D.V., and Gudasheva, T.A., *Pharm. Chem. J.*, 2013, no. 1, pp. 20–27.
20. Jaouadi, M., Martinez, J., and Castro, B., *Org. Chem.*, 1987, vol. 52, pp. 2364–2367.
21. Ueda, Y., Walsh, E., Nakanishi, H., and Yoshida, K., *Neurosci. Lett.*, 1994, vol. 165, nos 1–2, pp. 203–207.
22. Alam, A., *Anal. Biochem.*, 1992, vol. 203, no. 1, pp. 121–126.
23. Towbin, H., Staehelin, T., and Gordon, J., *Proc. Natl. Acad. Sci. U. S. A.*, 1979, vol. 76, no. 9, pp. 4350–4354.
24. Kukhtina, V.V., Tsetlin, V.I., Utkin, Y.N., Inozemtseva, L.S., and Grivennikov, I.A., *J. Nat. Toxins*, 2001, vol. 10, no. 1, pp. 9–16.
25. Brown, R.F., Hui, K.Y., Matter, W.F., and Vlahos, C.J., *J. Biol. Chem.*, 1994, vol. 269, no. 7, pp. 5241–5248.
26. Alessi, D.R., Cuenda, A., Cohen, P., Dudley, D.T., and Saltiel, A.R., *J. Biol. Chem.*, 1995, vol. 270, no. 46, pp. 27489–27494.
27. Siren, A.L., Fratelli, M., Brines, M., Goemans, C., Casagrande, S., Lewczuk, P., et al., *Proc. Natl. Acad. Sci. U. S. A.*, 2001, vol. 98, no. 7, pp. 4044–4049.
28. Hathway, G.J. and Fitzgerald, M., *J. Pain*, 2006, vol. 7, no. 1, pp. 57–61.

Translated by L.Onoprienko